

## Designing and optimization of different types of graded lattice structures of turbine blade

Osamah Abdulhameed<sup>a\*</sup>

<sup>a</sup> Industrial Engineering Department, College of Engineering and Architecture, Al-Yamamah University, Riyadh-11512, Saudi Arabia

### ARTICLE INFO

#### Article history:

Received 15 July 2024

Accepted 19 January 2025

Available online

19 January 2025

#### Keywords:

Lattice structures

Additive manufacturing

Topology optimization

Tripily Periodic Minimum

Surface (TPMS)

Finite Element Analysis

### ABSTRACT

Additive manufacturing by direct metal fabrication represents one of the fastest-growing areas in material science and manufacturing. Modern manufacturing demands that parts be engineered to have high strength, be lightweight with complex geometrical details, and be suitable for operation upon completion. A very good example of such engineering-manufacturing involves the design and manufacturing of turbine blades for energy efficiency. On the other hand, topology-optimized lattice structures have huge potential and flexibility available to designers operating in the area of designing lightweight structures and high-strength ones at the same time, in contrast to solid form structures. The key issues involved in the research include designing graded density structures made from different lattice architectures for dense materials by characterization of the thermo-mechanical properties for a number of lattice settings in Gyroid, Diamond, Schwarz, Lidinoid, Split P, and Neovius lattices for varied parameters. This paper questions how appropriately the design structure functions in high-speed-rotating elements, such as turbine blades. The current research work will be aimed at the design, finite element analysis for simulation, and manufacturing through additive manufacturing of the turbine blades, considering several designs and lattice structures that satisfy the requirements of lightweight construction and high strength. A detailed preliminary design study has already been performed with the aim of justifying the idea presented in this paper and to create an initially validated basis. It therefore presents findings from the design of different lattice structures, supported by simulations that explain the potential, extent, and limitations of the proposed paper with regard to its general scope.

## 1. Introduction and literature review

Lattice structures in materials would form due to the configurations of the unit cells in monotonic materials. Configuration is normally set along a specific spatial pattern dictated by the unit cells of the material. The nature and orientation of these lattice structures go a long way in determining the mechanical properties of engineering materials. One characteristic feature of the lattice structure is its porosity. A system of lattices can thus be defined as a combination of different types/configuration of lattices. Therefore, this would allow much more flexibility on the part of the designers in creating and engineering such materials that can have relatively high strength at low weight, particularly compared to structures with much lower porosity in their design. The optimization of thrust-to-weight ratio and minimum consumption of fuel are some of the keen interests in industries dealing with automotive and aerospace (Tang, Kurtz, & Zhao, 2015; Cutolo, Engelen, Desmet, & Van Hooreweder, 2020). It is for these two reasons that such designs creep into being more lucrative. Building up the challenge of the lattice structure lies in how to reduce the weight of the turbine blade without giving up the structural integrity of withstanding high temperatures and efficient dissipation. The production of lightweight lattice frameworks characterized by intricate geometries, along with suitable research and development (RD) and material compositions, can be achieved through additive manufacturing (AM) methods (Saleh, Anwar, Al-Ahmari, & Alfaify, 2022; Thompson et al., 2016). Such techniques can also be used in the creation of lattice structures which would have unique mechanical, thermal, and optical properties. Shi et al. (2020), for instance, performed tests on different kinds of structures created by SLM at different

\* Corresponding author.

E-mail addresses: [o\\_abdulhameed@yu.edu.sa](mailto:o_abdulhameed@yu.edu.sa) (O. Abdulhameed)

densities. They designed and tested Gyroid, Diamond, IW, and Primitive designs of lattice structures for compression effectiveness and energy absorption. The research on lattice structures is something that many industries-majorly those having to do with aerospace and medicine-are keenly watching. Lattice structures are quite needed in such a way that they can reduce weight while the mechanical and physical properties in a component can easily be controlled (Tang et al., 2015; Cutolo et al., 2020). Besides, lattice structures allow design flexibility not needing an overall change in structural form (Yonekura, Hattori, & Nishizu, 2023; Duan, Wen, & Fang, 2020). This property has been considered a key motivation toward using lattice structures in the production of turbine blades. Whatever the method used in developing the required crystalline lattice structure within the material, the homogeneity within it and its packing has to be ensured first and foremost. This is considered one of those techniques, which can ensure said homogeneity within. It results from a study presented in (Alkebsi, Ameddah, Outtas, & Almutawakel, 2021) where the authors have used AM for producing blades with graded lattice structure instead of a fully solid structure. In the case of a graded lattice structure, better mechanical and physical properties were reported in comparison to the solid structures. The topological interactions among lattices and the constituting material of its components are greatly responsible for enhancement in the end-use characteristics of blades (Al-Ketan, Al-Rub, & Rowshan, 2018). In relation to the material lattice, however, the finding of the Optimal lattice configuration is the first determining factor to be considered. Amongst all, the Diamond, Gyroid, and primitive structures have been determined as the three most efficient lattice configurations by the scholars. All these variants are basically based on the very basics of TPMS, which is an abbreviation for triply periodic minimal surface. With its optimum topological properties, designing TPMS involves the indulgence of mathematical sciences through mathematical equations that take part in the formulation and fabrication of different surfaces. Equations relating to the design of TPMS are known as “level-set-approximation equations” (Al-Ketan et al., 2018). The latter case is then grouped to obtain the 3D lattice structure (Shokrani, Dhokia, & Newman, 2012). Also, quite a number of additive manufacturing parts undergo machining operations such as a grinding operation to get the desired geometrical tolerances. The general trend is that machining operations are generally difficult, especially in instances where the parts are made of hard-to-machine materials like Ti6Al4V and Inconel 718, among other super alloys (Cheng et al., 2019). The process of machining, more precisely grinding, is very reliant on the build orientation of the part, layer formation, and lattice structure. The anticipated lattice structure from this research will be totally new. Thus, the attempt is to:

1. Design different parametric lattice patterns for a lightweight blade design.
2. Optimization of the turbine blade design in detail for minimum weight with least mechanical thermal stresses/deflection.
3. The verification of the design through the EBM fabrication of turbine blades.

## 2. Methodology

It would therefore be very application-dependent due to the nature of the approach towards the lattice structure design, which, by choice of appropriate geometry, involves manifold parameters such as cell dimensions, shell thickness, lattice thickness, and mesh tolerance. Once the geometry is established, thermomechanical behavior for the blade is studied under various conditions, and then the design parameters are adjusted to achieve the desired result. This process involved testing the structure in a virtual environment using finite element analysis. It is an FEA-based simulation analysis of unit cells built through 3D extrusion. The analysis is carried out through the use of nTop commercial software and periodic boundary conditions are used to perform this analysis. The methodology is as shown in Fig. 1.

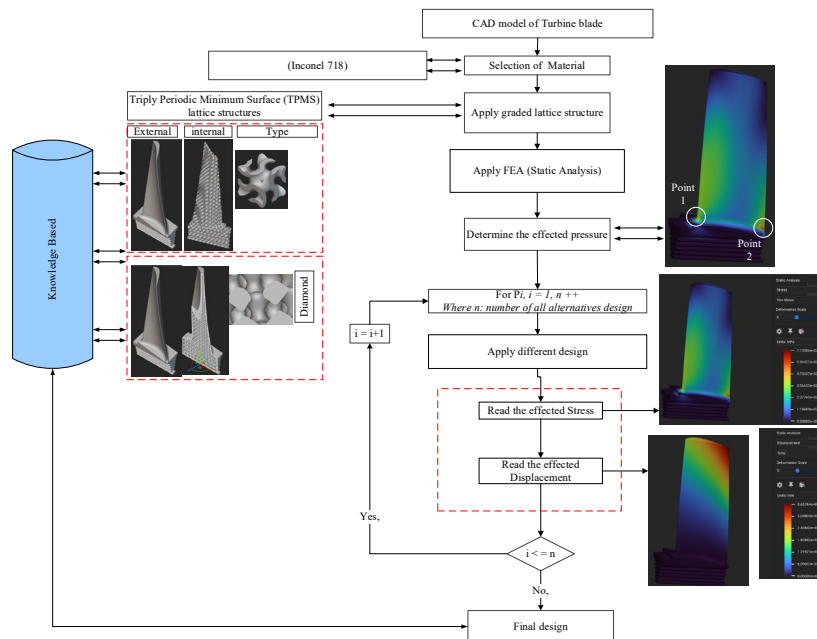
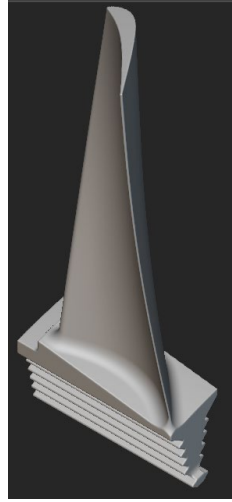


Fig. 1. Methodology of the graded lattice structure

### 3. Design phase

The first step involves the designing and optimization of lattice structures having uniformity in the design. The design is associated with the 3D model of a turbine blade as shown in **Fig. 2**. Coordinates of the blade profile are used to design the blade. NACA (NACA 2412 (naca2412-il)) data has been used to produce the similar model design with original mass equal to 289g.



**Fig. 2.** Turbine blade

The lattice optimization is applied using nTop software by combining structural lattices with Additive Manufacturing, mechanical design engineers can achieve unprecedented weight reduction, increasing part performance, saving material and reducing manufacturing costs. The purpose is to get a reduced mass and constraints of stresses. As explained in the literature review, the optimization requires to have homogeneity between the lattice structures and its associated parameters, therefore, in this paper the homogeneity method has been applied which is reported by (Cheng et al., 2017; Ludwig, Rabold, Kuna, Schurig, & Schlums, 2020). Following are the mathematical equations used for the optimization under the said method:

The structures and its associated parameters, therefore, in this paper the homogeneity method has been applied which is reported by Cheng et al. (Cheng et al., 2017; Ludwig et al., 2020) Following are the mathematical equations used for the optimization under the said method:

$$\min m(\rho) = \sum_{e=1}^N \rho_e v_e$$

$$w.r.t. \quad \rho_e$$

$$\text{such that } \begin{cases} KU = F^{in} \\ \bar{C} = \bar{C}(\rho) \\ \sigma_{max}^H(\rho) \leq 1, \\ \underline{\rho} \leq \rho_e \leq \bar{\rho}, \quad e = 1, \dots, N \end{cases}$$

where,

$m(\rho)$  = Objective function corresponding to volume mass of the designed lattice structure.

$\rho_e$  = Relative density of the material element  $e$  used in the design

$v_e$  = Volume of the material element  $e$  used in the design.

$K$  = Global stiffness matrix

$U$  = Global displacement vector

$F$  = External loads

$\bar{\sigma}_{max}^H$  = Maximum stress in the design domain

$$\max_{e=1:nN} \left( \frac{-H}{e} \right) \leq 1 = \text{Modified stress on the material element } e \text{ used in the design.}$$

$\gamma$  = Safety factor

$\sigma\gamma$  = Bulk material's yeild strength

$\rho$  = Minimum allowable design variable for the optimization

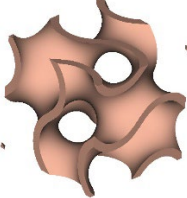
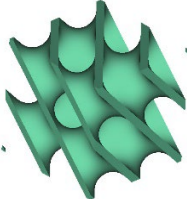
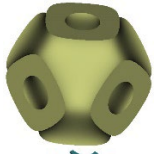
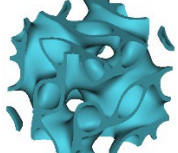
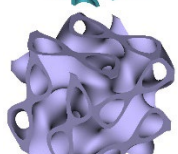
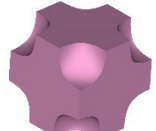
$\bar{\rho}$  = Maximum allowable design variables for the optimization.

The above equation consists of another constraint named as the scaling law of elasticity during the design of lattice structure. All the variables, constants and other related calculations are to be followed by the guidelines of homogeneity method (Sun et al., 2019).

#### 4. Design parameters

In the context of designing and optimization, various lattice structures under the primary domain of Triply Periodic Minimum Surface (TPMS) are designed and optimized where TPMS is the mathematical representation of a periodic volume in implicit form. The first step in producing lattice structures is piling up different unit cells upon each other along the direction of primary axes such as x, y, and z, axis, as shown in **Table 1**. These lattice structures are created by placing unit cells in a certain pattern in space. The performance characteristics of the entire lattice structure is reflected in and determined by the various types of unit cells due to their distinctive properties.

**Table 1.** Different configurations of lattice structures and equations:

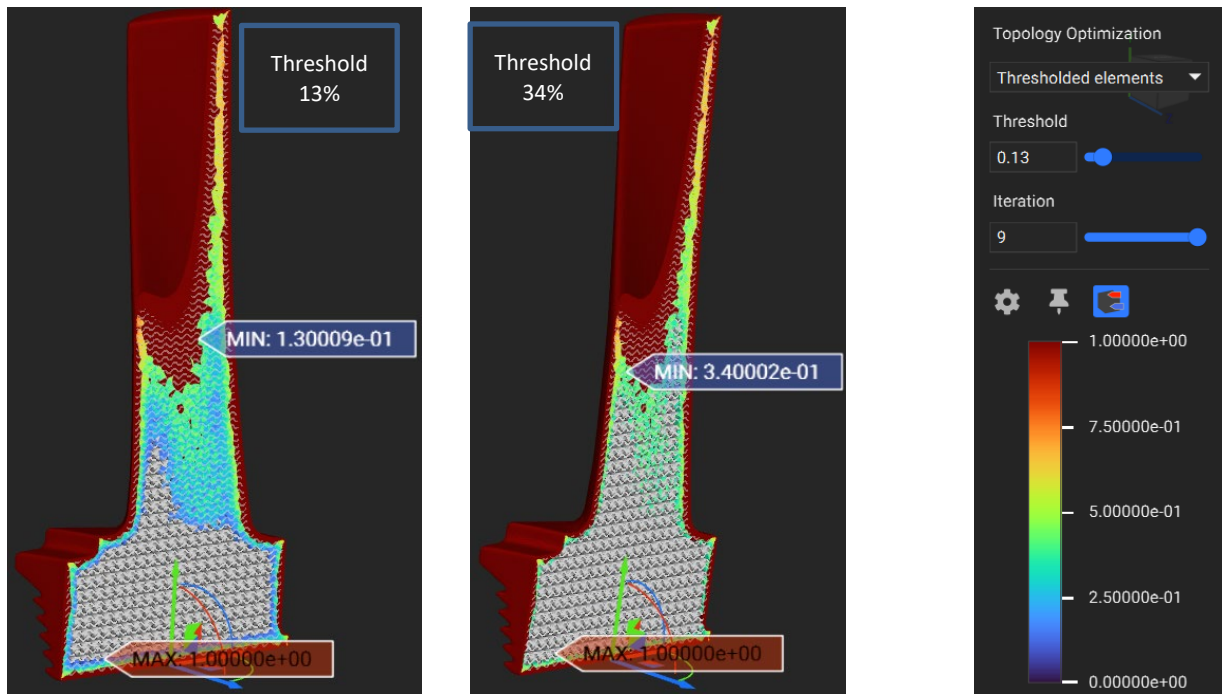
Lattice type	Level-set approximation equation	Graphical representation
Gyroid	$\sin(x) \cos(y) + \sin(y) \cos(z) + \sin(z) \cos(x)$	
Diamond	$\sin(x) \times \sin(y) * \sin(z) + \sin(x) * \cos(y) * \cos(z) + \cos(x) * \sin(y) * \cos(z) + \cos(x) * \cos(y) * \sin(z)$	
Schwarz	$\cos(x) + \cos(y) + \cos(z)$	
Lidinoïd	$\sin(2*x) * \cos(y) * \sin(z) + \sin(2*y) * \cos(z) * \sin(x) + \sin(2*z) * \cos(x) * \sin(y) - \cos(2*x) * \cos(2*y) - \cos(2*y) * \cos(2*z) - \cos(2*z) * \cos(2*x) + 0.3$	
Split P	$1.1 * (\sin(2*x) * \sin(z) * \cos(y) + \sin(2*y) * \sin(x) * \cos(z) + \sin(2*z) * \sin(y) * \cos(x)) - 0.2 * (\cos(2*x) * \cos(2*y) + \cos(2*y) * \cos(2*z) + \cos(2*z) * \cos(2*x)) - 0.4 * (\cos(2*x) + \cos(2*y) + \cos(2*z))$	
Neovius	$3 * (\cos(x) + \cos(y) + \cos(z)) + 4 * \cos(x) * \cos(y) * \cos(z)$	

The different combinations of parameters of TPMS design type, lattice thickness, and cell size applied to the original design as shown in Table 2.

**Table 2.** Design parameters

Types of Lattice Thickness	Lattice Thickness (unit)	Cell size (unit)
Gyroid	1	5
	2	10
	15	15
Diamond	1	5
	2	10
	15	15
Schwarz	1	5
	2	10
	15	15
Lidinoïd	1	5
	2	10
	15	15
SplitP	1	5
	2	10
	15	15
Neovius	1	5
	2	10
	2	15

The combination of the Gyroid TPMS with 5mm cell size and 1mm lattice thickness parameter resulted model as shown in Fig. 3.

**Fig. 3.** TPMS (5mm cell and 1mm thickness) of Gyroid structure

## 5. Material properties

According to (Wang et al., 2019) the turbine's parts must be able to meet strong thermomechanical actions. Different materials, particularly nickel-base superalloys, because of their extraordinary capacity to endure both mechanical and thermal stresses, so that it can reflect the real environment of the gas turbines and their other allied conditions (Nagesh, Apoorva, & Mohan, 2017).

**Table 3.** Inconel 718 Set of different properties required in case of designing the turbine blades.

Property	Unit	Value
Density	Kg/m <sup>3</sup>	8190
Young's Modulus	GPa	200
Ultimate Tensile Strength	MPa (min)	1375
Yield Tensile Strength	MPa	1100
Thermal Conductivity	w/m <sup>o</sup>	11.4
Specific Heat	J/Kg <sup>o</sup> C	435
Capacity Melting Point	<sup>o</sup> C	120-1336
The Bulk Modulus	MPa	1.375e+5
Shear Modulus	MPa	63,463
Poisson's Ratio		0.3

The authors of the current study recommend employing Inconel 718 material to design and fabricate a turbine blade having various lattice structures of graded design in place of solid structure having full infill density throughout its entire shape, specifically the inner volume. It is resistant to wear, has a high electric resistance, good thermal conductivity, high hardness, and good chemical stability. In this way, Inconel 718 finds favor and has been in application as the main material for turbine blades in a gas turbine engine. Some of its important characteristics are shown in **Table 3**, which include the physical and mechanical properties. The optimization result and comparison from different combinations of parameters of TPMS design type comparing with original design (it's mass equal to 289g) as shown in **Fig. 4**:

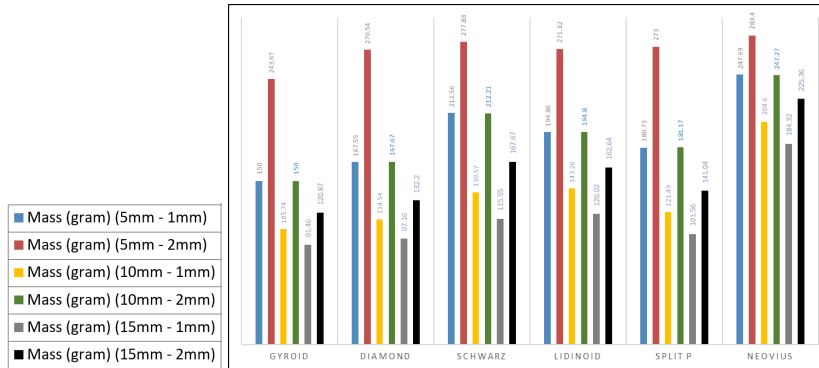


**Fig. 4.** Comparison of mass reduction in gram for every parameter

## 6. Boundary conditions

Land-based state-of-the-art gas turbines are being operated at about 1370°C compared to their counterparts operating at a temperature of 820°C according to (Sun et al., 2019). Inconel 718 had resistance to high temperature up to 1350°C and many other thermal-related problems arising in gas turbines. This is one of the reasons that Inconel 718 has been used in many gas turbine variants. Related literature, as well as the authors of the proposed manuscript, preferred Inconel 718 for use in turbine blades. Some operating parameters of gas turbines were also obtained from research work in (Sun et al., 2019), which analyzed some of the thermal and mechanical properties of Inconel 718. Thus, the mesh in **Fig. 4** would represent one of the results of such a simulation, with 693,080 faces and 346,542 vertices with an average edge length of 1 millimeter, making easier the post-processing phase related to thermal and mechanical analyses of turbine blades.

The methodology taken into consideration for the FEA-based analytical study included advances in gas turbine technology and properties of the studied material, Inconel 718. The work hence according to (Nagesh et al., 2017) that, in general, the metastable state of current gas turbines is at a higher operating temperature of 1370°C compared to earlier models at 820°C. In this analysis, the local thermo-mechanical properties of the surroundings are brought into consideration to attain realistic operating conditions of the gas turbine. This is the reason why, in this regard, high temperature-resistant Inconel 718 was chosen to provide the material composition along the blade up to 1350°C. The FEA boundary conditions are collected from research by (Sun et al., 2019), where these authors have given most of the common operating boundary conditions of the gas turbines. Geometrical model of turbine blades Total discretization = 693,080 faces and 346,542 vertices. General size = 1 mm. Typical view of the mesh structure is shown in **Fig. 5**. This turbo mesh is very detailed and has served to create the wanted and appropriate simulations and predictions of the thermo-milieu analysis of the turbine blade. In general, correct thermo-mechanical behavior studies of Inconel 718 turbine blades operating at 1370°C require the application of realistic boundary conditions to the FEA model. In fact, the boundary conditions should ideally represent the operating loads and constraints of the blades. The following boundary conditions have been applied:

- Prescribed heat flux/temperature boundary conditions: A total of 1370 °C temperature value was applied on the surface of the blade. It is the temperature relevant to the hot gas temperature in gas turbines.
- Displacement boundary condition: Root of the blade is constrained along all three basic axes, viz. x, y, and z, to reflect the restraint provided by the turbine shaft.
- The pressure boundary condition is that pressure at the blade surface is kept constant and equals 10 bar, representing the pressure of hot gas crossing a turbine. These boundary conditions were applied to the FEA model using nTop. The model was then solved to obtain the stresses, strains, and displacements of the blade. It is important to note that the boundary conditions used in this study are simplified representations of the actual loads and constraints that the blades experience in a gas turbine. However, these boundary conditions are sufficient to provide valuable insights into the thermo-mechanical behavior of the blades at high temperatures. For example, the results of the FEA analysis can be used to predict the hot spots on the blade surface and to assess the risk of fatigue failure. The results can also be used to design more efficient and durable turbine blades for high-temperature applications. The mesh used in the study consisted of 693,080 faces and 346,542 vertices with an average

size of 1 mm. This mesh was sufficiently fine to capture the complex geometry of the turbine blade and to accurately represent the thermo-mechanical behavior of the blade at high temperatures.

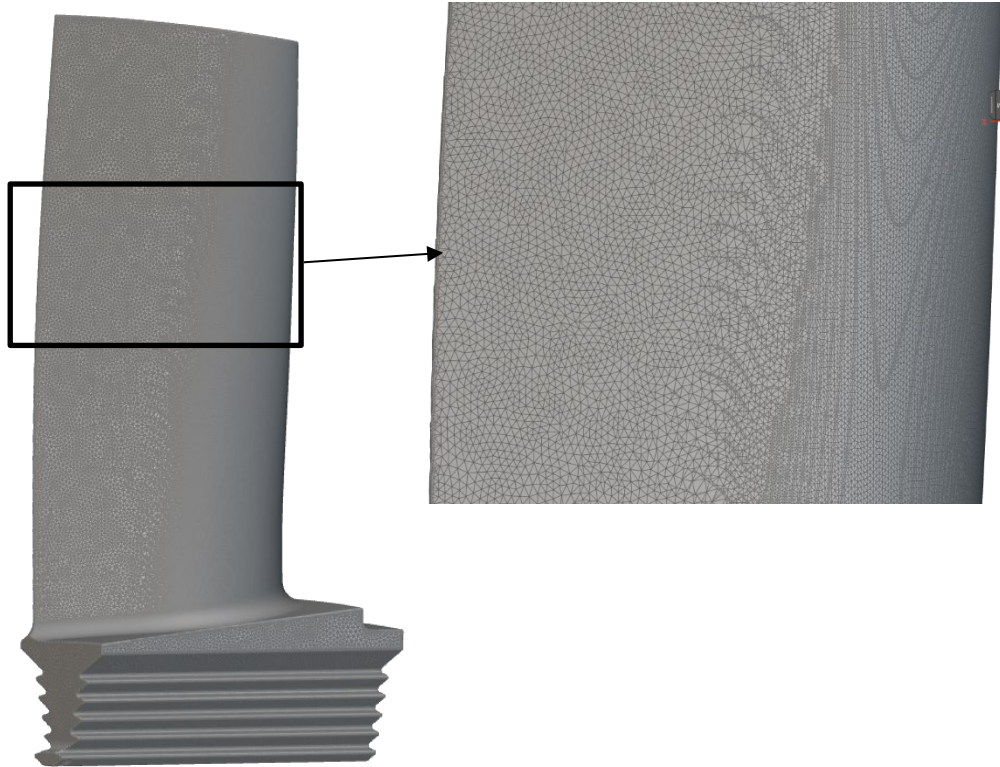


**Fig. 5.** Generated mesh at mesh tolerance 1 mm

The preliminary design of the turbine blade is analyzed in terms of its behavior under thermal and mechanical loading conditions. The analysis of both cases of the designs is performed in two stages. During the first stage the thermal loading conditions are taken such as the hot jet of steam targeting the blade’s edge. The detail can be seen in **Table 4** and **Fig. 6**. During the second stage of analysis thermo-mechanical load was considered. All degrees of freedom were eliminated, particularly for the embedded part at the bottom of the blade which is fixed to the root. In this way the mechanical, e.g. static structural analysis was performed to see the collective effect of thermal and mechanical loading. Thermal loading was extracted from the first stage whereas the mechanical load was calculated due to the applied steam pressure at the tip point of the blade.

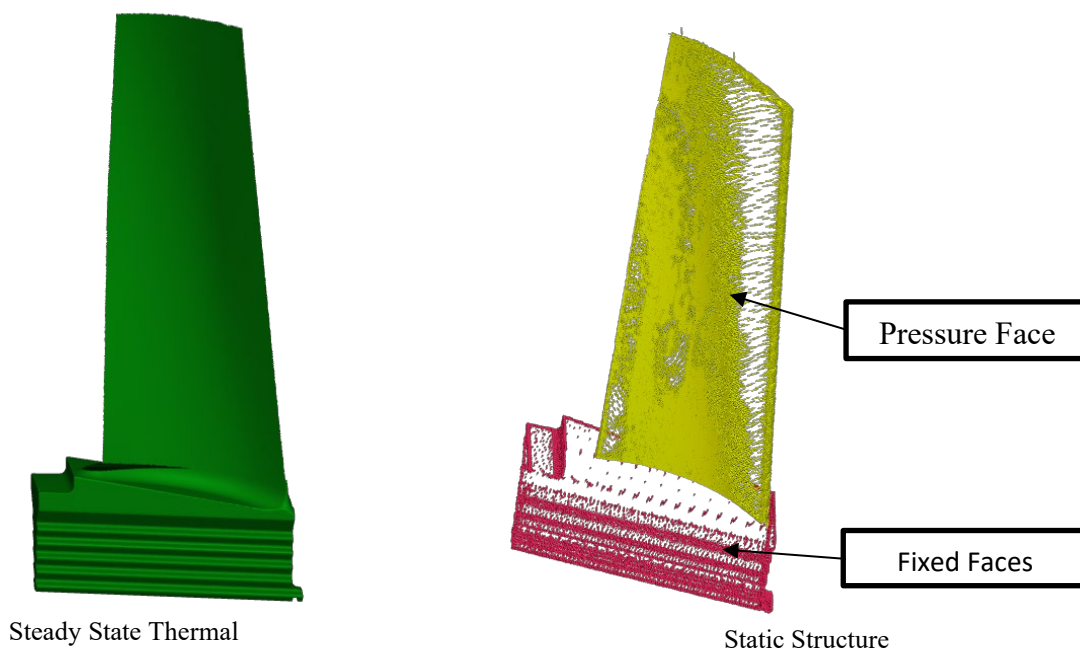


**Fig. 6.** Steady state of turbine blade

**Table 4.** Some of the loads applied on the turbine blades (thermal loads and mechanical loads).

Parameters	Value
Pressure	10 MPa
Heat transfer coefficient	0.000025 W/mm <sup>2</sup> °C
Ambient temperature	1350°C
Initial temperature	350°C

**7. Results**

In the following sections, the initial results of the design blade configured through FEA are explained and presented. The results are found to be highly encouraging in the context of fabrication and meeting the set objectives which are mainly to design and fabricate light weight structures of the turbine blade.

*7.1 Initial Results: Infill of turbine blade*

Total Heat Flux (Max  $3.57 \times 10^6$  W/m<sup>2</sup> W/m<sup>2</sup>), Stress (Max 1006.18 MPa) and the mechanical deflection in the form of deformation is changed from a value of 0 to a maximum level of 3.56 mm. Please refer to **Table 5**.

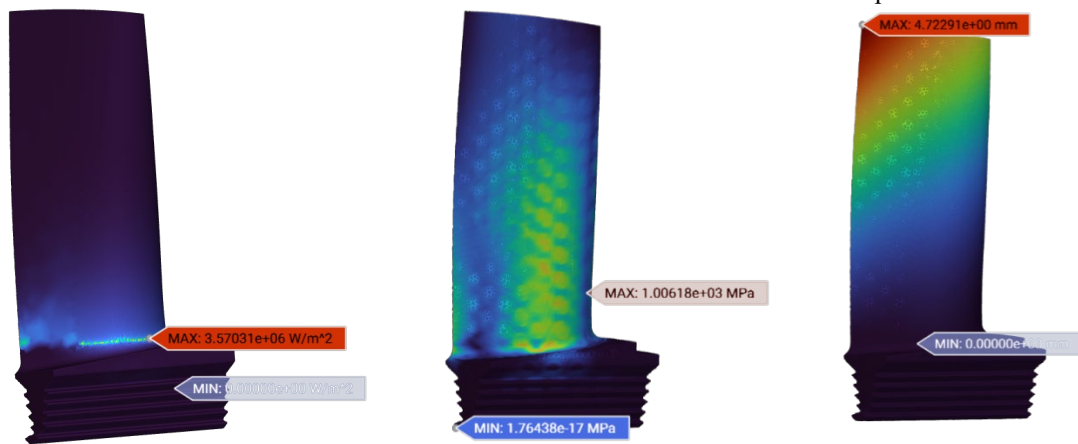
**Table 5.** Results of the initial design of the blade

Original part Heat Flux =  $3.57 \times 10^6$  W/m<sup>2</sup>

Stress = 1006.18 MPa

Displacement = 3.56 mm

Mesh  
Tolerance = 1  
  
Mass = 289 g



*7.2 Initial Results: lattice Structure Designs*

Here six different designs of the lattice structure are already attempted and explain in the forthcoming paragraph and tables. The designs include:

- 1. Gyroid design
- 2. Diamond Design
- 3. Schwarz Design
- 4. Lidinoid Design
- 5. Split P Design
- 6. Neovius Design

In this stage, a comparison between different designs, which were obtained from the last module, to determine the optimal selection of parameters, which are TPMS, lattice thickness and cell size has been extensively carried out.

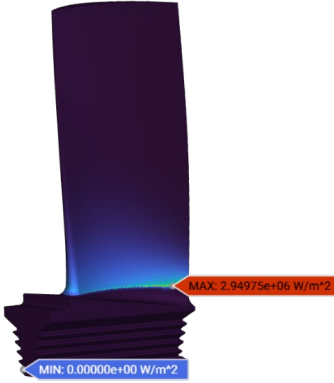
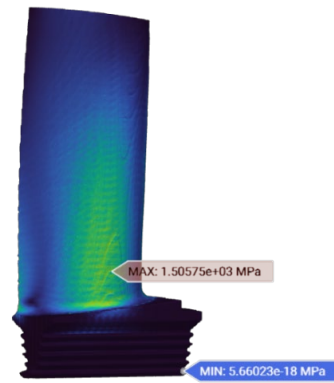
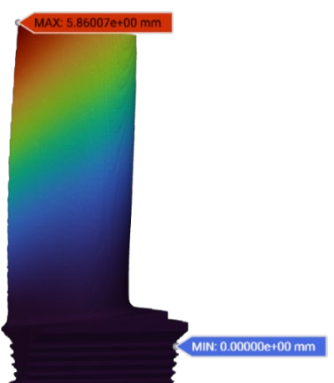
**Table 6.** Gyroid TPMS at all parameters of cell size and lattice thickness.

Parameters	Heat Flux W/m <sup>2</sup>	Stress	Displacement (Min. & Max.)
Gyroid:			
Cell size = 5 X 5 X 5			
Lattice thickness = 1			
Shell thickness = 2			
Mesh Tolerance = 1			
Mass = 289 g			

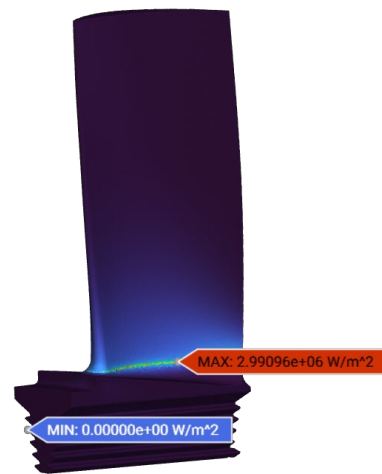
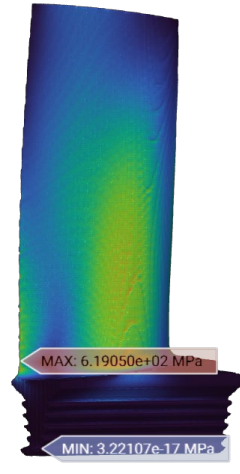
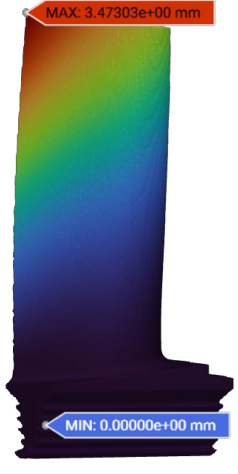


It can be considered as the initial level validation of the proposed designs and their efficacy. The above stated lattice design structures are designed by topology optimization technique at ntopology software and some of the selected designs are presented in **Table 6**, **Table 7**, **Table 8**, **Table 9**, **Table 10**, and **Table 11**. These tables illustrate the design parameters for each of the above listed designs, the heat flux values, stress, and displacements analysis. The study of numerical simulations of the suggested lattice structures under the influence of the thermomechanical loads conducted as follows:

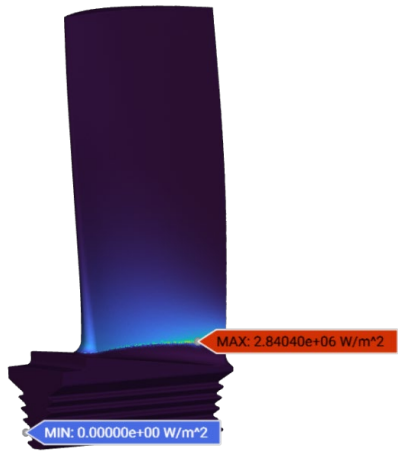
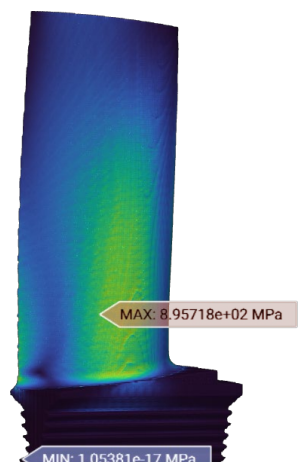
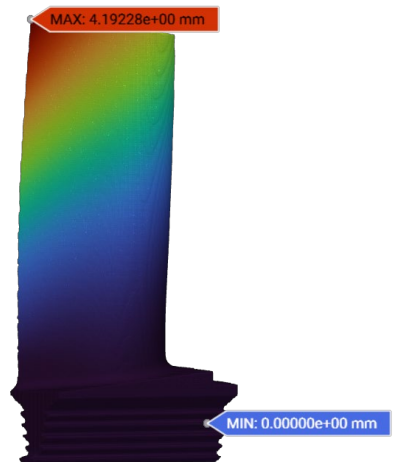
**Table 7.** Diamond TPMS at all parameters of cell size and lattice thickness

Parameters	Heat Flux W/m <sup>2</sup>	Stress	Displacement (Min. & Max.)
Diamond:			
Cell size = 5 X 5 X 5			
Lattice thickness = 1			
Shell thickness = 2			
Mesh Tolerance = 1			
			

**Table 8.** Schwarz TPMS at all parameters of cell size and lattice thickness:

Parameters	Heat Flux W/m <sup>2</sup>	Stress	Displacement (Min. & Max.)
Schwarz:			
Cell size = 5 X 5 X 5			
Lattice thickness = 1			
Shell thickness = 2			
Mesh Tolerance = 1			
			

**Table 9.** Lidinoid TPMS at all parameters of cell size and lattice thickness:

Parameters	Heat Flux W/m <sup>2</sup>	Stress	Displacement (Min. & Max.)
Lidinoid:			
Cell size = 5 X 5 X 5			
Lattice thickness = 1			
Shell thickness = 2			
Mesh Tolerance = 1			
			

**Table 10.** SplitP TPMS at all parameters of cell size, and lattice thickness:

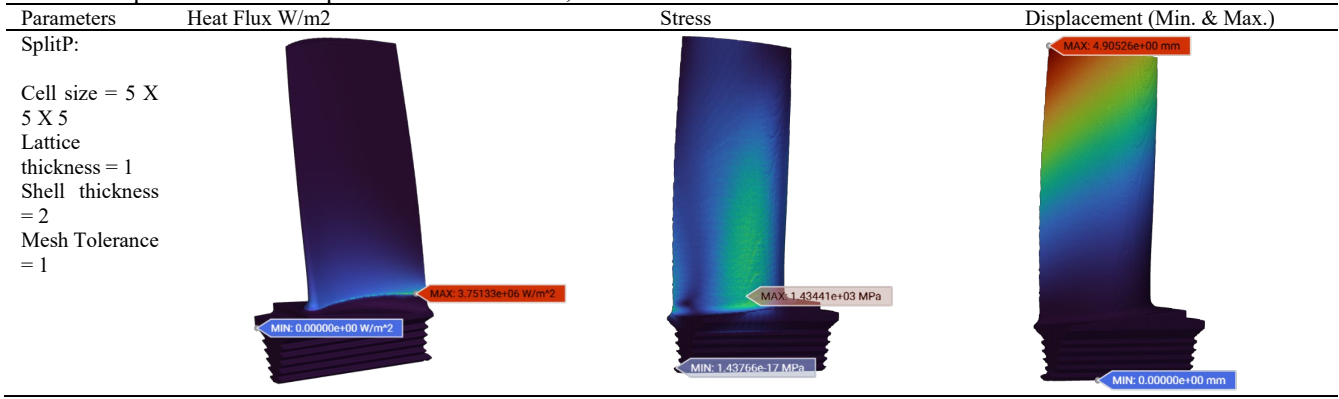
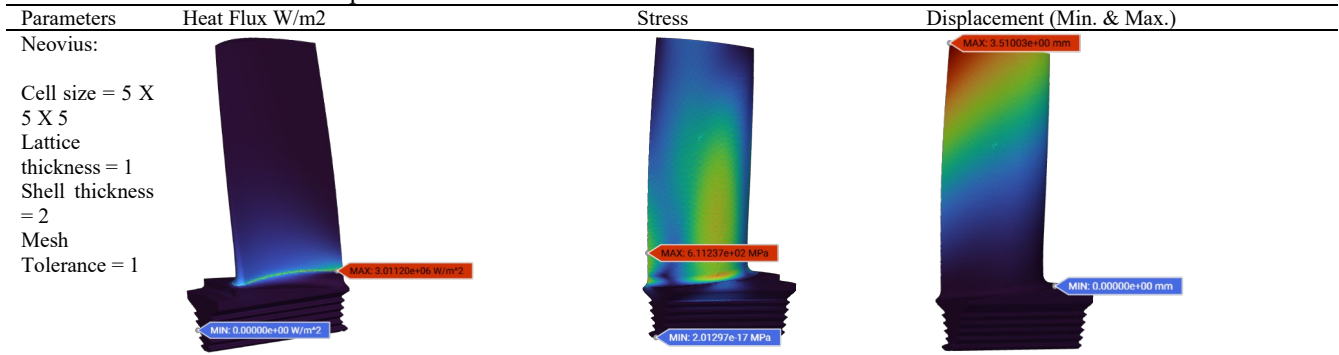


**Table 11.** Neovius TPMS at all parameters of cell size and lattice thickness:



7.3 Comparative Design Analysis of Thermo-mechanical properties

The graph-based analysis is done for various parameters of cell dimensions and thickness of the lattice for different configurations of TPMS lattices depicted in Figs. (7-12).

7.4 Comparative Design Analysis (5mm cell and 1mm Lattice Thickness)

A comparison across all the designs for TPMS lattice configurations for 5mm cell and 1mm lattice thickness design indicates that Schwarz meets the criteria for minimum heat flux rate across it, with the minimum induced stress and consequently displacement.

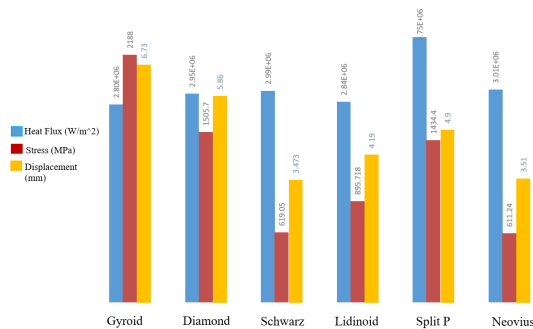


**Fig. 7.** TPMS (5mm cell & 1mm thickness)

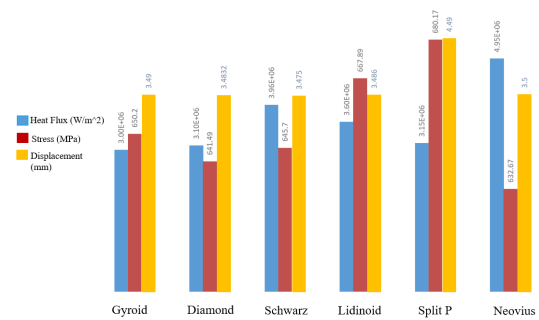


**Fig. 8.** TPMS (5mm cell & 2mm thickness)

7.5 Comparative Design Analysis (5mm cell and 2mm Lattice Thickness)

A comparison among all the TPMS lattice configurations with a cell size of 5 mm and a lattice thickness of 2 mm reveals Diamond configuration for desired characteristics. The Diamond configuration has ensured the low value of heat flux, stress, and displacement.

7.6 Comparative Design Analysis (10mm cell and 1mm Lattice Thickness)

By comparing various lattice configurations of TPMS at the cell size of 10 mm with a lattice thickness of 1 mm, one can realize that the Neovius configuration has good properties like low values of heat flux, stress, and displacement.

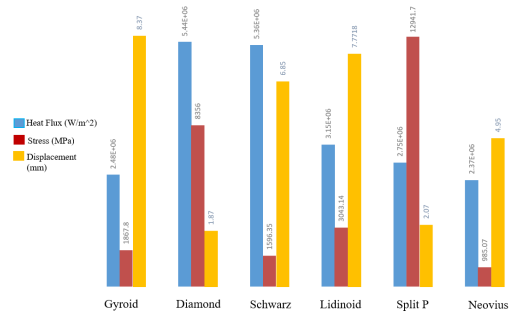


Fig. 9. TPMS (10 mm cell & 1mm thickness)

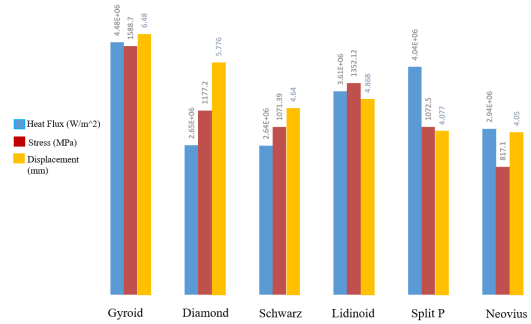


Fig. 10. TPMS (10mm cell & 2mm thickness)

7.7 Comparative Design Analysis (10mm cell and 2mm Lattice Thickness)

Comparison of all TPMS lattice structures at cell size 10 mm and 2mm Lattice thickness. Neovius design shows the possession of properties like low value of heat flux, stress and displacement.

7.8 Comparative Design Analysis (15mm cell and 1mm Lattice Thickness)

Comparing these different TPMS lattice structures at a cell size of 15 mm and a lattice thickness of 1 mm, good characteristics have been released for the Schwarz configuration in terms of the lower magnitude of heat flux, stresses, and displacements.

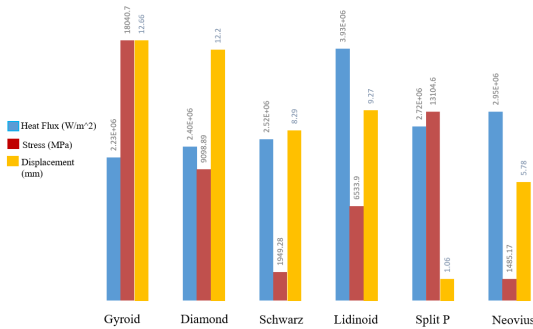


Fig. 11. TPMS (15mm cell & 1mm thickness)

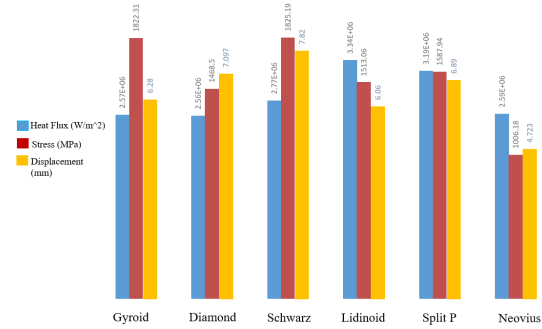


Fig. 12. TPMS (15mm cell & 2mm thickness)

7.9 Comparative Design Analysis (15mm cell and 2mm Lattice Thickness)

Comparison performed for all TPMS lattice structures for cell size 15mm and Lattice Thickness of 2mm: The required properties can be concluded from neovius design as minimum value of heat flux, stress and displacement.

7.10 Properties Comparison

Finally, a Comparison between stresses, heat fluxes, and displacements of all TPMS lattice structures as shown in Figs. 13-15.

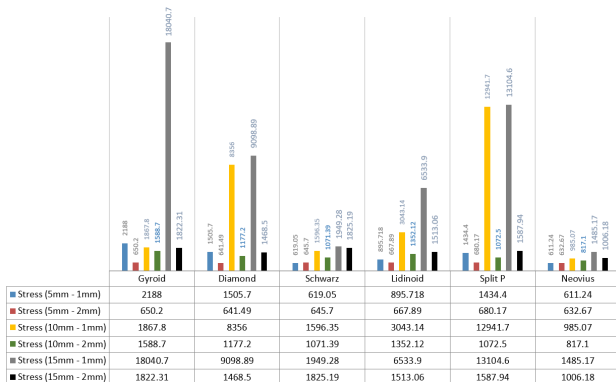


Fig. 13. Comparison between Stresses of all TPMS lattice structures

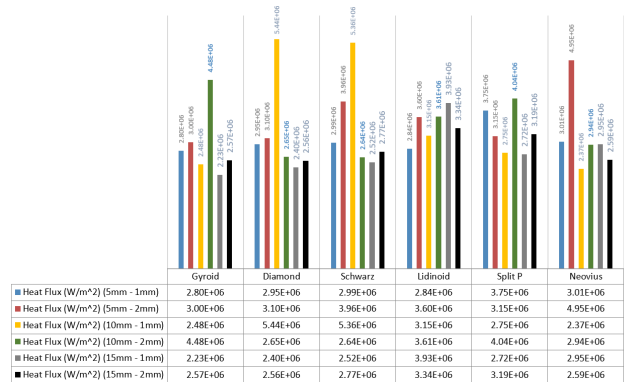


Fig. 14. Comparison between heat fluxes of all TPMS lattice structures

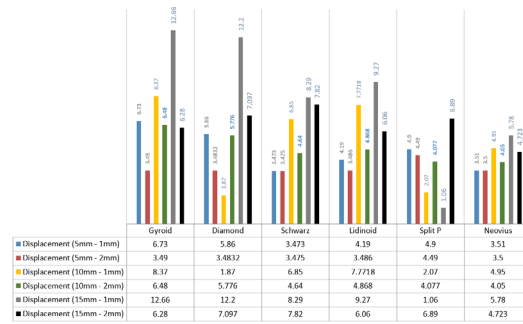


Fig. 15. Comparison between displacements of all TPMS lattice structures:

## 8. Conclusion

This research paper has a wide range of applications as discussed in the literature such as light weighting of aerospace components, overall structure weight reduction, significant reduction in the consumption of energies involved in the entire process (during the manufacturing of the components as well the energy consumption of the overall machine structure). Testing of new materials alternate, testing of new structure parameters, and testing of material mechanical and thermal properties through simulation will help to identify the most appropriate materials and component structures to result into lightweight engineering components (like turbine blades) and energy efficiency in the manufacturing processes. Therefore, the proposed design structure is really a light weight having the same or better thermos-mechanical properties as compared to the conventionally used design structures and their corresponding properties.

## References

- Al-Ketan, O., Al-Rub, R. K. A., & Rowshan, R. (2018). The effect of architecture on the mechanical properties of cellular structures based on the IWP minimal surface. *Journal of Materials Research*, 33(3), 343-359.
- Alkebsi, E. A. A., Ameddah, H., Outtas, T., & Almutawakel, A. (2021). Design of graded lattice structures in turbine blades using topology optimization. *International Journal of Computer Integrated Manufacturing*, 34(4), 370-384.
- Cheng, L., Liang, X., Bai, J., Chen, Q., Lemon, J., & To, A. (2019). On utilizing topology optimization to design support structure to prevent residual stress induced build failure in laser powder bed metal additive manufacturing. *Additive Manufacturing*, 27, 290-304.
- Cheng, L., Zhang, P., Biyikli, E., Bai, J., Robbins, J., & To, A. (2017). Efficient design optimization of variable-density cellular structures for additive manufacturing: theory and experimental validation. *Rapid Prototyping Journal*, 23(4), 660-677.
- Cutolo, A., Engelen, B., Desmet, W., & Van Hooreweder, B. (2020). Mechanical properties of diamond lattice Ti-6Al-4V structures produced by laser powder bed fusion: On the effect of the load direction. *Journal of the Mechanical Behavior of Biomedical Materials*, 104, 103656.
- Duan, S., Wen, W., & Fang, D. (2020). Additively-manufactured anisotropic and isotropic 3D plate-lattice materials for enhanced mechanical performance: Simulations & experiments. *Acta Materialia*, 199, 397-412.
- Ludwig, C., Rabold, F., Kuna, M., Schurig, M., & Schlums, H. (2020). Simulation of anisotropic crack growth behavior of nickel base alloys under thermomechanical fatigue. *Engineering Fracture Mechanics*, 224, 106800.
- Nagesh, R., Apoorva, H., & Mohan, R. (2017). Static structural analysis of gas turbine blades comparing the materials, *Int. Adv. Res. J. Sci. Eng. Technol.*, 2394-1588.
- Saleh, M., Anwar, S., Al-Ahmari, A. M., & Alfaify, A. (2022). Compression performance and failure analysis of 3D-printed carbon fiber/PLA composite TPMS lattice structures. *Polymers*, 14(21), 4595.
- Shi, X., Liao, W., Li, P., Zhang, C., Liu, T., Wang, C., & Wu, J. (2020). Comparison of Compression Performance and Energy Absorption of Lattice Structures Fabricated by Selective Laser Melting. *Advances in Engineering Materials*, 22, 1-9, doi:10.1002/adem.202000453.
- Shokrani, A., Dhokia, V., & Newman, S. T. (2012). Environmentally conscious machining of difficult-to-machine materials with regard to cutting fluids. *International Journal of machine Tools and manufacture*, 57, 83-101.
- Sun, W., Bhowmik, A., Tan, A. W. Y., Xue, F., Marinescu, I., Li, F., & Liu, E. (2019). Strategy of incorporating Ni-based braze alloy in cold sprayed Inconel 718 coating. *Surface and Coatings Technology*, 358, 1006-1012.
- Tang, Y., Kurtz, A., & Zhao, Y. F. (2015). Bidirectional Evolutionary Structural Optimization (BESO) based design method for lattice structure to be fabricated by additive manufacturing. *Computer-Aided Design*, 69, 91-101.
- Thompson, M. K., Moroni, G., Vaneker, T., Fadel, G., Campbell, R. I., Gibson, I., . . . Ahuja, B. (2016). Design for Additive Manufacturing: Trends, opportunities, considerations, and constraints. *CIRP annals*, 65(2), 737-760.
- Wang, X., Hui, Y., Hou, Y., Yu, Z., Li, L., Yue, Z., & Deng, C. (2019). Direct investigation on high temperature tensile and creep behavior at different regions of directional solidified cast turbine blades. *Mechanics of Materials*, 136, 103068.
- Yonekura, K., Hattori, H., & Nishizu, T. (2023). Fluid topology optimization and additive manufacturing of a liquid atomizer using an extensive number of grid points: Minimizing pressure loss of liquid atomizer. *The International Journal of Advanced Manufacturing Technology*, 126(3-4), 1799-1806.

